Melanin Zinc Complex as a Biocompatible Agent for Clearing Bacteremia

Tahmineh Rahmani Eliato, Seth Edwards, Zhen Tian, Cheryl P. Andam, Kyung Jae Jeong,* and Young Jo Kim*

Sepsis, whole-body inflammation caused by the contamination of blood by bacteria and endotoxins, affects millions of patients annually with high mortality rates. A recent promising approach to treat sepsis involves the removal of bacteria and endotoxins using extracorporeal blood-cleansing devices. However, poor specificity, slow recognition of pathogens, and high costs remain the main limitations. Here, the melanin, a biologically derived pigment, is reported for the rapid binding of bacteria and endotoxins from the contaminated blood. This novel approach utilizes the specific binding between Zn2+-loaded melanin and bacteria/endotoxins with minimal nonspecific interactions with human blood components. Melanin contains various chemical functional groups that allow reversible chelation of metallic ions such as Zn2+ via redox reactions. Zn2+ enables rapid and specific binding with bacteria/endotoxins due to the strong electrostatic interactions between Zn²⁺ and phosphate ions. The presence of various zinc-binding proteins on the bacterial cell membrane further enhances the binding. The well-known biocompatibility and low cost make melanin an ideal material to interface with human blood. Zn2+-charged melanin can remove 90% of E. coli and 100% of endotoxin in PBS and human blood. Zn2+-melanin also demonstrated excellent hemocompatibility shown by protein adsorption, blood coagulation, and hemolysis tests.

1. Introduction

Sepsis is a severe whole-body inflammation caused by an uncontrolled immune response to bacterial infection of the blood, often

T. R. Eliato, S. Edwards, Z. Tian, K. J. Jeong, Y. J. Kim
Department of Chemical Engineering
University of New Hampshire
Durham, NH 03824, USA
E-mail: kyungjae.jeong@unh.edu; youngjo.kim@unh.edu
C. P. Andam
Department of Biological Sciences
University at Albany
State University of New York
Albany, NY 12222, USA

The ORCID identification number(s) for the author(s) of this article can be found under https://doi.org/10.1002/admi.202300369

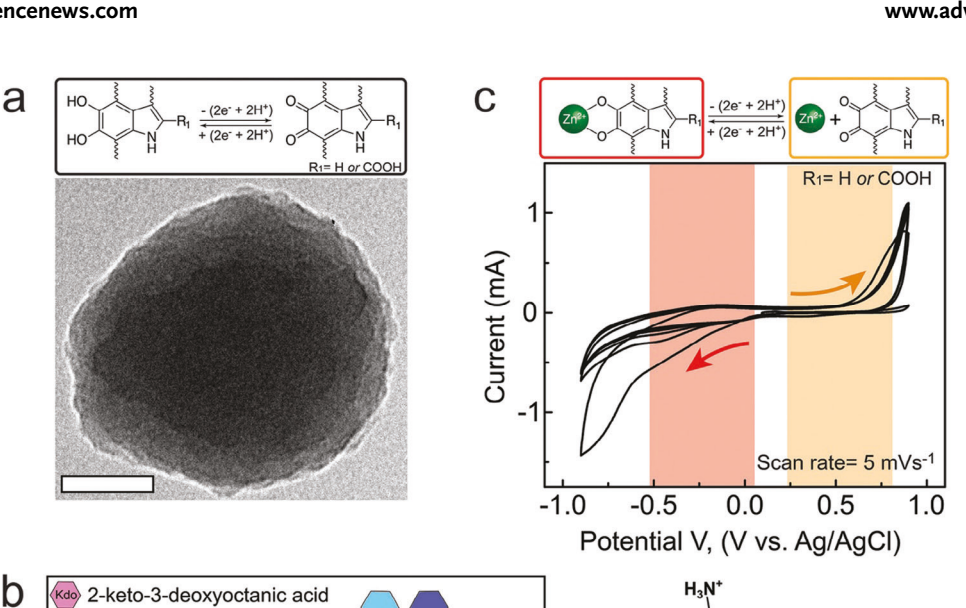
© 2023 The Authors. Advanced Materials Interfaces published by Wiley-VCH GmbH. This is an open access article under the terms of the Creative Commons Attribution License, which permits use, distribution and reproduction in any medium, provided the original work is properly cited.

DOI: 10.1002/admi.202300369

leading to organ dysfunction and even death.[1] Worldwide, 49 million cases of sepsis were reported each year, of which an estimated 11 million patients ultimately died from complications related to septic shock.[2] Due to an aging population, increased use of invasive procedures, and immunosuppressive therapies, including cancer chemotherapy and organ transplantation, sepsis has become one of the leading causes of death in adults and infants in the United States.^[3] Current therapies rely on the use of broad-spectrum antibiotics before the pathogen is identified, raising concerns for the disruption of natural microbiome balance and antimicrobial resistance.^[4] Even in the case of effective antibiotic therapy against gramnegative bacteria, the outer cellular membranes of dead bacteria release negatively charged and reactive endotoxins such as lipopolysaccharides (LPS).^[5] LPS can initiate the sepsis inflammatory cascade, resulting in multi-organ failure, septic shock, and death.^[6] Based on these

observations, targeted separation of LPS and the bacteria from the blood can complement conventional antibiotic therapy.

Successful removal of LPS and bacteria from the patient's blood can be accomplished using an extracorporeal blood-cleaning device that specifically targets the endotoxin and/or bacteria.^[7] Such devices include hemoperfusion and microfluidic-magnetic apparatuses which are designed to draw the patient's blood and selectively remove bacteria/endotoxins in the filtration unit.^[8] The filtration relies on the specific binding using antibodies, engineered proteins, or synthetic molecules incorporated in the membrane. [9] For example, antibodies against bacterial cell membranes were immobilized on the surface of magnetic micro/nanoparticles for the specific binding with bacteria in microfluidic devices.[3,10,11] In another study, an innate immune protein, mannose-binding lectin (MBL), was used for the recognition of bacteria and endotoxin. MBL was fused with the Fc region of the antibody and immobilized on a membrane surface to capture bacteria and endotoxin. [12] In another example, a zinc-chelating synthetic molecule, bis-dipicolylamine (bis-DPA), which mimics the structure of annexin V, was immobilized on magnetic nanoparticles for the rapid removal of bacteria and endotoxin from blood. [3] Despite the promising research and



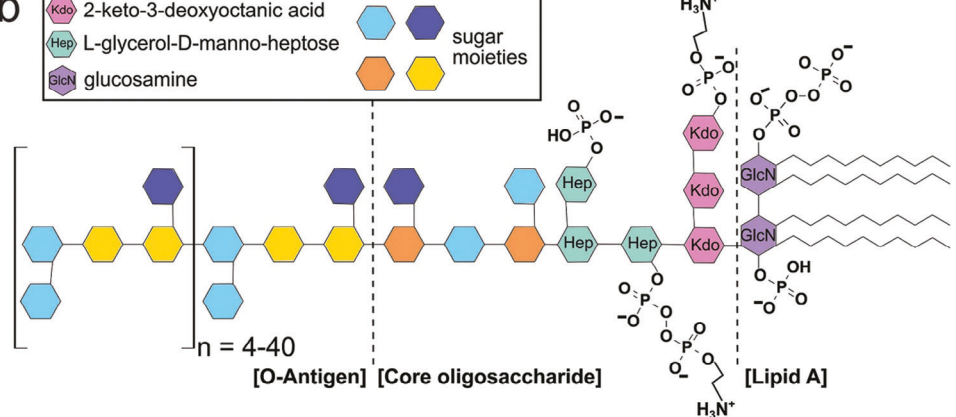


Figure 1. The microstructure of melanins is shown in (a) taken by transmission electron microscopy. The scale bar indicates 50 nm. b) Chemical structure of Lipopolysaccharide (LPS) from *E. coli* O111:B4. LPS is characterized by three main units: Lipid A, Core oligosaccharide, and O-antigen. Lipid A is critical to the endotoxin activity of LPS. $^{[25,26]}$ High density of negatively charged phosphate groups is observed in oligosaccharide and Lipid A regions. Zn ions are electrochemically incorporated in melanin using cyclic voltammetry (CV) over five cycles as shown in c). CV was performed in 0.5 M Zn(NO₃)₂ at a scan rate of 5 mV s⁻¹. The cathodic region corresponds to simultaneous Zn²⁺ removal and oxidation of catechols to o-quinones. Zn ions can form coordination bonding at the anodic region during the electrochemical reduction from o-quinone to catechol.

development, there are inherent limitations to these methods. The antibody-based methods have a very low separation speed as they rely on highly specific antibody-antigen interactions. Additionally, protein-based methods including the fused MBL are associated with high production costs due to the low yield and separation requirements and show challenges in storage and quality control.

Herein, we demonstrate that naturally occurring melanin pigments loaded with zinc ions may serve as active material in separating LPS and bacteria from blood. Melanins are a class of multifunctional biopolymers^[13] that can be readily obtained either by natural or synthetic routes at low costs. As the most ubiquitous form of melanins, eumelanins (hereafter called melanins for simplicity) are primarily composed of subunits of 5,6-dihydroxyindole (DHI) and 5,6-dihydroxyindole-2-carboxylic acid (DHICA) monomers in various ratios that are π -stacked to form homogeneous nanoparticles.^[14] It is highly biocompatible and has many favorable physical and chemical properties.^[15,16] Melanins contain diverse chemical functional groups includ-

ing pendant carboxylic acids, aromatic amines, and catechols.^[17] Redox-active catechols are oxidized into ortho(o)-quinones by losing two electrons, and two protons (Figure 1a).[18] During the redox reaction, catechols can form coordination bonding with protons, and ions.^[19] This electrochemical feature has enabled melanins to be used in aqueous charge storage devices with divalent cations.^[20] Here, we show a novel approach leveraging melanin redox reactions to immobilize zinc ions (Zn²⁺) and bind to bacteria and endotoxin from blood. Zn2+ largely exhibits a stronger affinity toward negatively charged molecules compared to other divalent cations, (e.g., Mg²⁺ or Ca²⁺) due to the presence of a filled d-orbital.^[21] Zn²⁺ plays an important role as an anion receptor in biological systems, particularly associated with phosphate derivatives.^[22] This property, initially described in metalloenzymes with high phosphate selectivity, allows phosphates to act as substrates or inhibitors by reversible binding to Zn2+ in the active site.^[23] The interactions between Zn²⁺ and phosphates have been utilized to develop biological assays to detect apoptotic cells and bacteria.[24,25] Subsequently, we hypothesize that



www.advancedsciencenews.com



www.advmatinterfaces.de

Zn²⁺-loaded melanins (Mel-Zn) would form ionic binding with anionic phospholipid groups in LPS that exists as either a component of the outer membrane of gram-negative bacteria or a freely circulating molecule. Our previous study has shown that natural melanin can be used as an antibacterial agent by generating reactive oxygen species via the redox reaction of catechol/oquinone. Given zinc binds with catechol groups, this study focuses on the selective binding of bacteria or LPS with Mel-Zn. Simple and cost-effective preparation of Mel-Zn along with rapid binding kinetics would make its clinical application plausible for the extracorporeal blood-cleansing device.^[26]

2. Results and Discussion

LPS is a major structural building block of the outer membrane of gram-negative bacteria. It contains a high density of anionic phospholipids and has been known to be a critical component in septic shock in humans.^[27] LPS is an amphipathic molecule with a general structure consisting of three defined regions: lipid A, core oligosaccharide, and O-antigen (Figure 1b). Lipid A is most often composed of a dimer of glucosamine (GlcN) attached to acyl chains (fatty acids) by ester or amide linkages and normally contains phosphate groups on each GlcN. [28,29] Lipid A is covalently attached to anionic groups, 2-keto-3-deoxyoctanic acid (Kdo) in the core region together with L-glycero-D-manno-heptose (Hep) and hexoses.^[28] The O-antigen is a repeating oligosaccharide unit, which determines the strain-specific serological identity of the respective bacterium.^[28] Although both the polysaccharide regions and lipid A can induce immune responses, the latter is the most immunogenic and considered the endotoxin center of LPS.[27] The core oligosaccharide of LPS largely consists of phosphorylated or phosphate-containing groups, such as pyrophosphate or 2-aminoethylphosphate. These groups assist in stabilizing the structure by increasing the negative charge of the cell membrane.^[30] We hypothesized that the rapid formation of ionic binding between these phosphates and Zn²⁺ would facilitate the separation of LPS.

Melanin extracted from *Sepia officinalis* exhibits homogeneous nanoparticle aggregates with a characteristic length of 80–120 nm in diameter (Figure 1a). Spherical microstructures contain layers of protomolecules that are π -stacked with an intermolecular spacing of 3.8 Å.^[31] The presence of ordered protomolecules of melanin in the meso scale has been corroborated by computational simulation.^[32–34] Catechols present in melanin can reversibly bind multivalent cations such as Mg²⁺, Ca²⁺, Fe^{2+/3+}, or Zn²⁺ by undergoing a redox reaction induced by two electrons and two protons.^[19] Catechols largely exhibit a stronger affinity for multivalent ions (0.95 eV) than oxidized σ -quinones (0.23 eV).^[35] Concerted redox reactions, differential cation binding affinity, and nanostructure collectively promote the multivalent ion insertion and release in melanins.^[19,20]

The electrochemical behavior of melanins in a Zn-containing solution was measured by cyclic voltammetry (CV, Figure 1c). No significant peak was observed from both anodic and cathodic regions, which contrasts with the electrochemical behavior of melanins in Mg-containing solution that showed prominent redox peaks. [20] This indicates that Zn^{2+} is incorporated with melanins in a capacitive manner. The incorporation of zinc ions

with melanin occurs when o-quinones of melanins are reduced by the addition of two electrons and two protons at the anodic region, generating Zn^{2+} -loaded melanin (Mel- Zn_{CV}). Conversely, in the cathodic region, Zn^{2+} is removed from melanins during the oxidation reaction from catechols to o-quinone. Running the multiple redox cycles assists in increasing the amount of zinc loading in melanin by making more catechols accessible during the repeated redox reaction. To compare the binding efficiency of electrochemically prepared Mel- Zn_{CV} , Zn^{2+} -loaded melanin was generated by incubating melanin in a zinc solution at 0.1 and 0.05 M, resulting in Mel- $Zn_{0.1}$, and Mel- $Zn_{0.05}$.

The successful loading of zinc ions in melanin was assessed by X-ray photoelectron spectroscopy (XPS) and Raman spectroscopy (Figure 2). The presence of zinc ions loaded in melanin was probed by comparing Zn 2p peaks in the XPS survey (Figure 2a). Mel- Zn_{CV} contained 8×10^{-3} Zn/C, which is approximately two times higher zinc density than Mel-Zn_{0.1} and Mel-Zn_{0.05} (Figure 2b). The prominent increase in the Zn/C atomic ratio can be compared to other zinc-biomaterial complexes. For instance, Mishra et al. developed zinc-carboxymethyl chitosan (CMC)–genipin containing ≈1% zinc that can be used for antibacterial and mildly antibiofilm.^[36] In addition, high resolution Zn 2p peaks shown in Figure 2c further confirm zinc coupling in melanin with defined peaks for Mel-Zn samples, which are absent in pristine melanin. Detailed peak positions of highresolution Zn 2p peaks are summarized in Table S1 (Supporting Information). High resolution Zn 2p XPS exhibits two peaks at around 1021 and 1045 eV. Doublet formation of Zn (Zn $2p_{3/2}$ and $Zn 2p_{1/2}$) corroborates the presence of Zn^{2+} , which can be found from the zinc in zeolite imidazolate framework.[37] This result aligns with our prior data which demonstrates an increase in zinc binding using CV in comparison to incubation in aqueous zinc

Pristine and Zn-loaded melanins show Raman spectra comparable to other sp²-hybridized carbon materials (Figure 2d). [39,40] Raman spectra were deconvolved into five peaks $(\alpha - \epsilon)$ corresponding to carbon-carbon bonds of melanin subunits, DHI or DHICA (Table S2, Supporting Information).[18] Peak shift comparison from Raman spectra has been used to evaluate the potential locations of ion loading in melanin subunits compared to the pristine melanin.^[20] All deconvolved peaks of Znloaded melanins demonstrated peak shifts. The highest peak shift was found from α , which corresponds to the carboxylic acid of DHICA (Figure 2e). This region can also be regarded as the location where the subunits are polymerized to form a macromolecule such as the tetramer shown in Figure 2f. Compared to the planar indole backbones, the polymer bond formed among the subunits can be considered to be relatively weak, which results in the highest peak shifts observed from the α band (Figure 2d). This suggests that Zn²⁺ binds to the catechol during electrochemical redox process by CV, promoting the structural reconfiguration in meso scale. Taken together, Zn-binding was corroborated by both XPS and Raman and higher density of Zn²⁺ occurred during electrochemical loading compared to the spontaneous loading in aqueous zinc solutions.

Rapid initiation of appropriate antibiotic therapy is critical for patients with sepsis or septic shock. A microbiologically confirmed diagnosis is necessary for pathogen targeted antibiotic therapy. However, because culture-based diagnostics require sev-

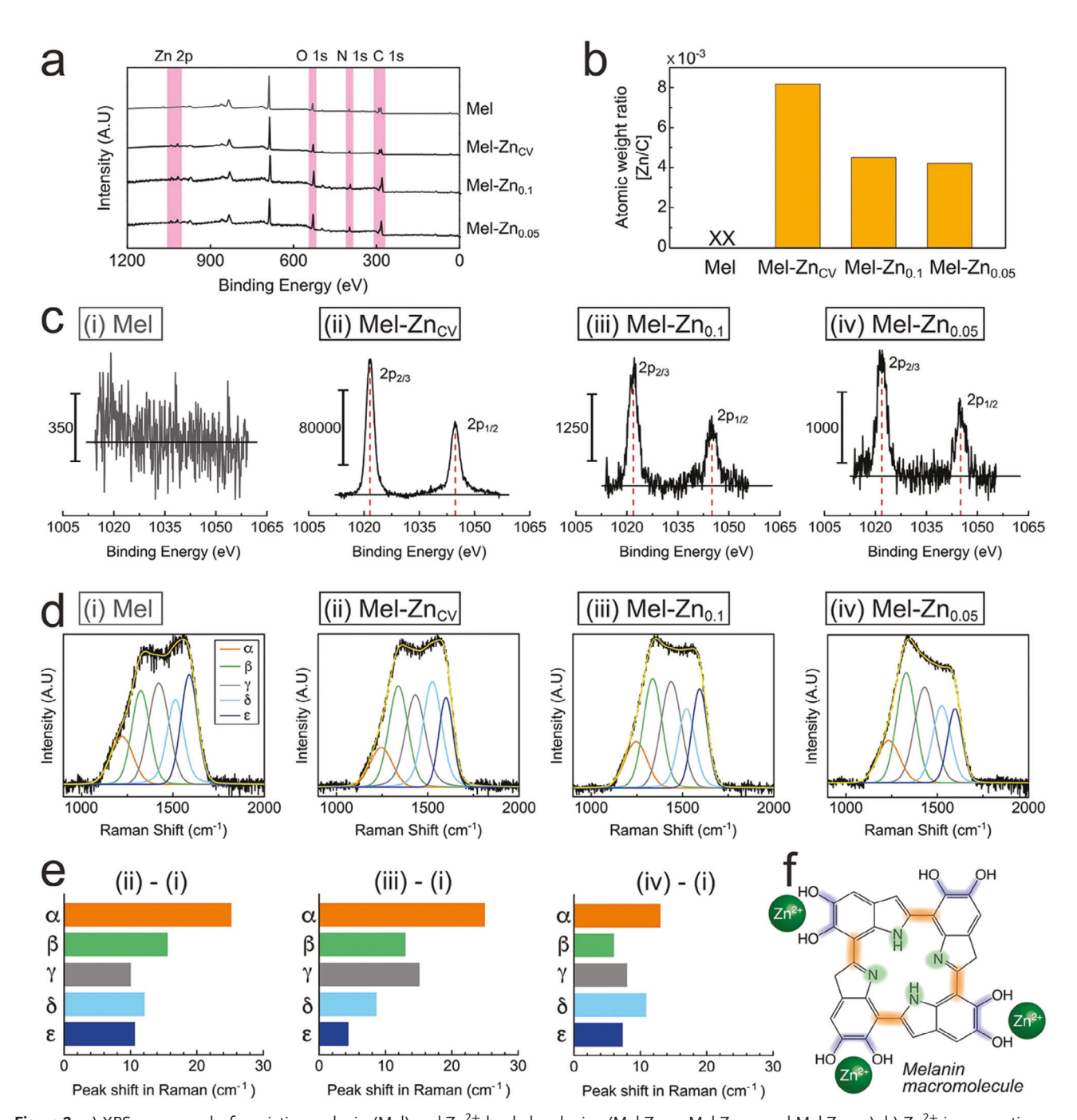


Figure 2. a) XPS survey peaks for pristine melanin (Mel) and Zn^{2+} -loaded melanins (Mel- Zn_{CV} , Mel- $Zn_{0.1}$, and Mel- $Zn_{0.05}$). b) Zn^{2+} incorporation was demonstrated by comparing the atomic weights of Zn 2p and C 1s peaks. Zn/C atomic weight ratio indicates Mel- Zn_{CV} exhibits \approx 2x higher binding density of Zn than Mel- $Zn_{0.1}$ and Mel- $Zn_{0.05}$. c) High-resolution XPS Zn 2p peaks show more detailed peak comparisons. d) Raman spectra of Mel and Mel-Zn are deconvolved into five bands (α - ϵ) using a Voigt function. Black lines represent the raw Raman spectra as recorded. Peak fitting and deconvolution were performed by CasaXPS and represented by different line colors. e) Peak shifts of (ii-iv) Mel-Zn relative to (i) Mel. This infers that the macromolecular structure of melanin is reconfigured in meso scale by Zn^{2+} loading. Detailed peak positions are summarized in tables S1 and S2 (Supporting Information).

eral days to be completed, broad-spectrum antibiotic therapy is often recommended as soon as possible after recognition of sepsis or septic shock.^[4] In cases of antibiotic-resistant pathogens, or to reduce the risk of antibiotic resistance development, direct removal of pathogens from the blood via purification tech-

niques could be an effective alternative strategy to treat septic patients. $^{[6,7,10]}$

Among culture-positive septic patients, 62.2% have gramnegative bacteria, of which, ≈20% are infected with *Escherichia coli*.^[41] Thus, an infection model of sepsis in PBS and whole

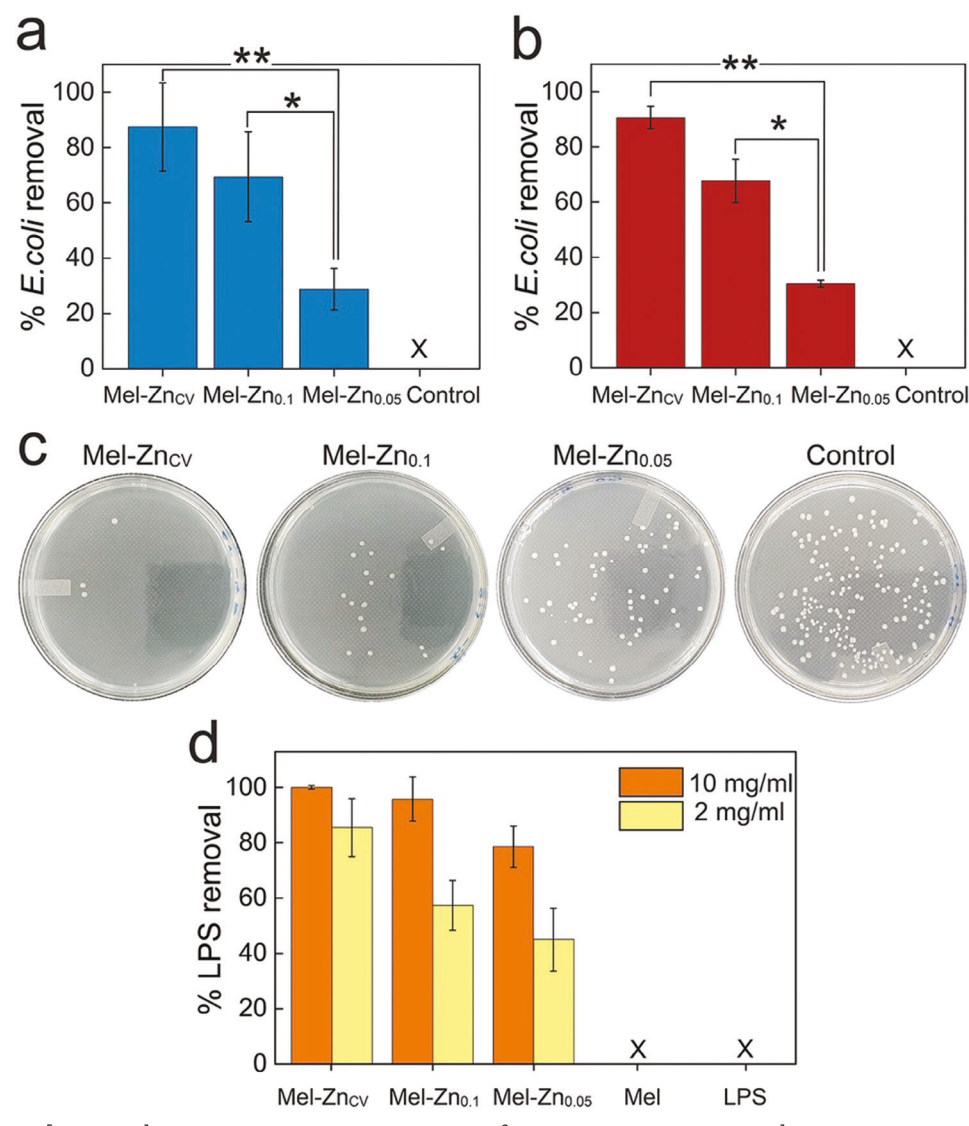


Figure 3. *E. coli* (5 × 10⁵ CFU ml⁻¹) binding efficiencies are shown for Zn²⁺-loaded melanins (5 mg ml⁻¹) after 1 h incubation in PBS solution a) and animal whole blood b) at 37 °C. Control shown here is the *E. coli* grown in pristine melanin. c) Digital images of agar plates after incubating Mel-Zn in animal whole blood with *E. coli*. d) LPS binding efficiencies are demonstrated after incubating two different concentrations of melanin (10 and 2 mg ml⁻¹) with 1 EU ml⁻¹ of LPS for 1 h at 37 °C. X indicates zero percent. Data are presented as mean \pm SD, n = 3. n.s., *, and ** represent the statistical significances of p > 0.05, p < 0.05, and p < 0.01, respectively.

blood was established using *E. coli* at a concentration of 5×10^5 CFU ml⁻¹ (CFU = Colony forming unit). Bacteria concentrations used in previous studies usually range from 10^4 to 10^7 CFU ml⁻¹. This study chose 5×10^5 CFU ml⁻¹ as the bacteria concentration which is within this range, which was also used from the previous study.^[3] Using higher concentrations of bacteria than what is found in vivo allows us to more robustly assess the effectiveness of the Mel-Zn complexes to remove the bacteria and LPS. Binding of *E. coli* from the PBS was studied by incubating Mel and Mel-Zn in *E. coli* solutions for 1 h and comparing the number of remaining *E. coli* with the negative control. As shown in Figure 3a, Mel-Zn_{CV} attained the highest efficiency of *E. coli* binding with $87.45 \pm 16\%$ in PBS while Mel-Zn_{0.1} and Mel-Zn_{0.05} showed $69.41 \pm 16.3\%$ and $28.82 \pm 7.4\%$ *E. coli* binding

efficiencies. The bacteria concentration in culture positive sepsis patients is much lower (1 to $10\,\text{CFU}\,\text{ml}^{-1}$) than the initial concentration used in this study. However, the culture-based methods of measuring these concentrations only account for live bacterial cells, which does not include the potential impact of dead bacteria or associated debris. In addition, using higher concentrations of bacteria than what is found in vivo allows us to more robustly assess the effectiveness of the Mel-Zn complexes to remove LPS. Accordingly, the concentration of pathogens in our study was selected to be higher than what would be seen in natural blood infection (1 to $10\,\text{CFU}\,\text{ml}^{-1}$). $[^{43,44}]$

Next, it was tested if Mel-Zn could remove bacteria $(5 \times 10^5 \text{ CFU ml}^{-1})$ from the whole blood environment during 1 h incubation. Mel-Zn_{CV} attained 90.6 \pm 4% binding of *E. coli*

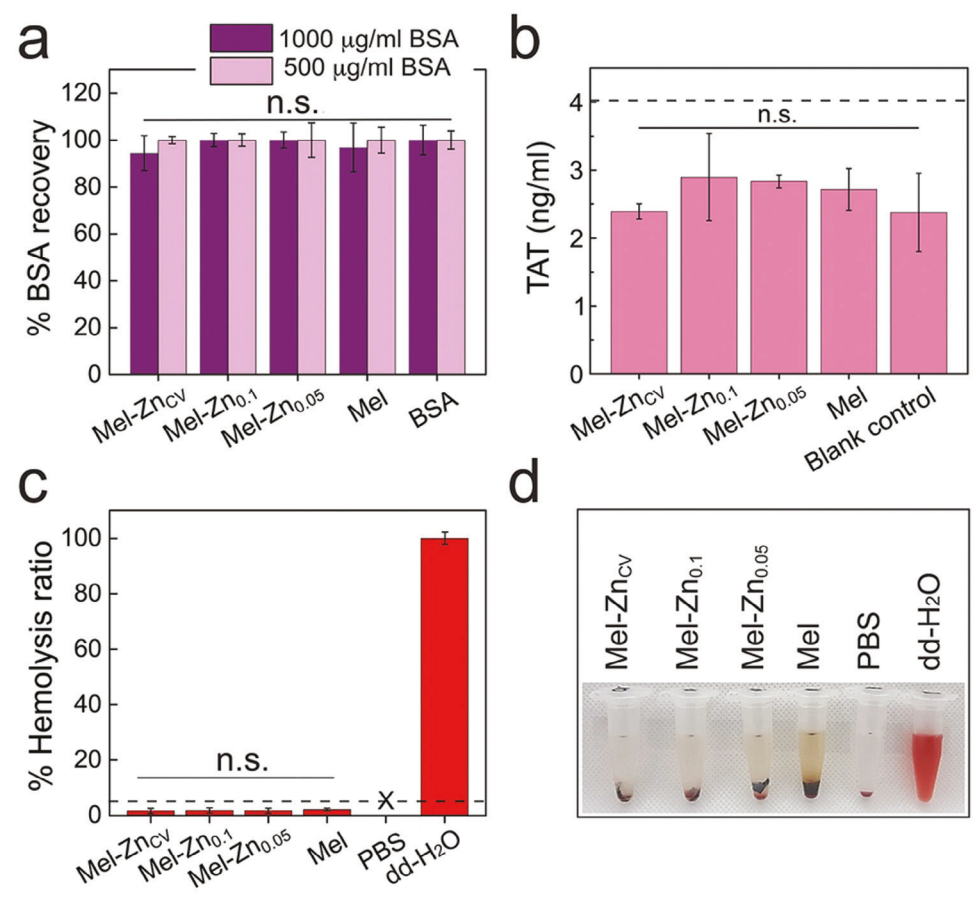


Figure 4. a) Blood compatibility is tested by BSA recovery after incubating melanins (5 mg ml⁻¹) within 1000 and 500 μg ml⁻¹ BSA for 1 h at 37 °C. Blood coagulation is tested by measuring thrombin antithrombin (TAT) complex levels. TAT levels are shown in b) after incubation of melanins in human blood for 30 min at 37 °C, which indicates no significant coagulation. The dashed line shows the normal upper limit of the TAT complex for healthy humans. [10] Hemolysis ratios are measured and shown in c) by incubating melanins (5 mg ml⁻¹) with human red blood cells (RBCs) at a concentration of 2 × 108 cell ml⁻¹ for 30 min. No severe damage to RBCs by melanins was observed. The dashed line shows the ASTM standard limit (5%) of hemolysis caused by biomaterials. [139,40] PBS and double-distilled H₂O were used as negative and positive controls, respectively. Digital images of RBC suspensions after incubation with melanin are shown in d). X indicates zero percent hemolysis. Data are presented as mean ± SD, n = 3. n.s., *, and *** represent the statistical significances of p > 0.05, p < 0.05, and p < 0.01, respectively.

while Mel-Zn $_{0.1}$ and Mel-Zn $_{0.05}$ achieved 67.69 \pm 7.9%, and 30.39 \pm 1.2% binding, respectively (Figure 3b). These results demonstrate that Mel-Zn can bind to bacteria in whole blood as well as PBS despite the more complex cellular and molecular compositions of the whole blood.

As gram-negative bacteria die under the antibiotic treatment, a large amount of LPS can be released into the blood. This could be highly detrimental as LPS can trigger the release of inflammatory cytokines that drive the sepsis cascade. As such, many patients do not respond to antibiotics alone since they only target the microbes. [6] Mel-Zn exhibits exceptional LPS binding efficiencies (Figure 3d). After 1 h incubation with LPS (1 EU mL $^{-1}$) in PBS, Mel-Zn $_{\rm CV}$ at concentrations of 10 and 2 mg ml $^{-1}$ removed 100% and 85.56 \pm 10.4% of LPS, respectively. Likewise, Mel-Zn $_{0.1}$ and Mel-Zn $_{0.05}$ at the higher concentration of 10 mg ml $^{-1}$ achieved LPS binding of 95.83 \pm 8% and 78.55 \pm 7.4%, respectively, while at 2 mg ml $^{-1}$ concentration, LPS binding was reduced to 57.35 \pm 8.9% and 44.99 \pm 11.3%, respectively. Notably, a high concentration of Zn $^{2+}$ promoted the removal of LPS or

 $E.\ coli$, corroborating the hypothesis that binding is mediated through LPS and Zn^{2+} interaction. The utility of melanin as an antibacterial agent has been investigated, however, the removal of bacteria/LPS by Mel-Zn will be more advantageous for the treatment of sepsis.

Hemocompatibility is a basic requirement for biomaterials that interface with human blood. The hemocompatibility of Mel-Zn was tested by protein adsorption, blood coagulation, and hemolysis (**Figure 4**). Protein adsorption on biomaterials can initiate the undesirable blood coagulation cascade, which can ultimately be fatal. [45] Protein adsorption on Mel-Zn was studied by incubating Mel-Zn in an aqueous solution of bovine serum albumin (BSA), the most prevalent protein in the human blood (\approx 54 mg ml⁻¹). Minimal BSA adsorption on Mel-Zn was observed regardless of the amount of zinc loading when melanin was incubated in 1000 and 500 µg mL⁻¹ BSA in PBS for 1 h (Figure 4a and Figure S1, Supporting Information), which is consistent with the earlier reports on melanin-based biomaterials. [46] Low protein adsorption might be due to the hydrophilic groups



www.advancedsciencenews.com



www.advmatinterfaces.de

in melanin such as carboxylic and hydroxyl groups and water molecules forming a hydration layer that prevents the protein adsorption.

Blood coagulation on Mel-Zn was investigated by measuring thrombin-antithrombin III (TAT) complex levels in the blood after the incubation with Mel-Zn for 30 min at 37°C. TAT complexes are rapidly formed through antithrombin III-mediated neutralization of thrombin and, therefore can be used as a proxy for thrombin concentration. No significant TAT complex formation was detected in all melanin groups compared to the negative control (p > 0.05) (Figure 4b). The TAT complex levels generated by Mel and Mel-Zn are well below the upper limit of 4.1 ng ml⁻¹ for a healthy human, Indicating exceptional hemocompatibility. This result is in accordance with plasma protein adsorption analysis that indicates no significant protein loss due to the introduction of Mel and Mel-Zn.

Excellent hemocompatibility of Mel-Zn was further confirmed by hemolysis tests. Hemolysis ratios were calculated after incubating 5 mg ml⁻¹ of melanins with red blood cells (RBC, 2×10^8 RBC ml⁻¹) for 30 min. [48,49] As indicated in Figure 4c,d the hemolysis ratios for Mel, Mel-Zn_{CV}, Mel-Zn_{0.01}, and Mel-Zn_{0.05} were 2.18%, 1.65% 1.83%, and 1.74%, respectively. These hemolysis ratios are much lower than the maximum limit permitted (5%) for biomaterials, according to ASTM F756-13 standards. [45,46] This indicates that Mel-Zn can be used to remove LPS or pathogens from sepsis blood effectively with minimal nonspecific interaction with RBCs. One limitation of this study is that the incubation time for the TAT assay and hemolysis test (30 min) was not the same as that of E. coli and endotoxin-binding tests (1 h). However, this incubation time has been used in many previous examples to verify the hemocompatibility of bloodinterfacing materials.[50-52] Our results still confirm that Mel-Zn is a promising hemocompatible biomaterial that can be used for sepsis treatment.

3. Conclusion

For the removal of bacteria and endotoxin from septic patients, the antibody-modified surface has been widely used due to their high specificities for their binding targets. However, there have been inherent limitations regarding poor separation speed, high production costs, and poor biocompatibility/hemocompatibilities. This study demonstrated the utility of Zn2+-loaded melanin as an active agent to bind bacteria and endotoxin. Melanin, a naturally occurring bio pigment is highly biocompatible and has many favorable features for the physiological systems. Melanin contains various chemical functional groups including pendant carboxylic acids, aromatic amines, and redox-active catechols. Electrochemical Zn²⁺ loading allowed the maximum loading density of Zn2+ into melanins compared to the solution method. XPS and Raman analysis corroborated that the loading of Zn²⁺ is largely associated with catechol groups. Zn²⁺-loaded melanin was found to remove approximately 90% of E. coli from PBS and whole blood, and 100% of endotoxin from PBS after 1 h incubation. Moreover, adsorption of protein from a protein model solution was found to be minimal. In addition, while antibiotic therapies leave behind LPS as cellular debris, the ability of Mel-Zn to bind to either LPS or bacteria could enhance the efficacy of antibiotics. Hemolysis and coagulation assays demonstrated the exceptional blood biocompatibility of Mel-Zn. Taken together, melanin would be a promising agent when implemented in an extracorporeal filtration unit to remove pathogens and endotoxins in acute sepsis patients.

4. Experimental Section

Preparation and Characterization of Mel-Zn: Melanin isolated from Sepia officinalis (Sigma-Aldrich, St. Louis, MO USA) was suspended in ethanol (5 wt.%) and sonicated using 80 W of power for 5 min using a probe sonicator (Digital Sonifier SFX 550, Branson, Brookfield, CT USA). Melanin suspension was filtered using filter paper (Grade 41, Whatman, Fisher Scientific, Pittsburgh, PA USA) and dried at 100°C for 2 h in a vacuum oven. Polytetrafluoroethylene (PTFE) (Good Fellow, Cambridge, England)) was blended with melanin in a 2:8 mass ratio using an agate mortar and pestle (Mel). Zinc ion (Zn²⁺) loaded melanin was prepared using electrochemical, and solution methods. Melanin (70 mg) was pressed into a stainless steel mesh current collector (Type 304, McMaster-Carr, Cleveland, OH USA) using a hydraulic press (P = 4 metric tons). A threeelectrode cell was configured with melanin, platinum wire, and Ag/AgCl as working, counter, and reference electrodes, respectively. A multichannel potentiostat-galvanostat (VMP3, Biologic, Knoxville, TN USA) was used to measure Cyclic voltammetry (CV) profiles. CV experiments were performed in the aqueous electrolyte of 0.5 M Zn(NO₃)₂ at a scan rate of $5~\text{mV}~\text{s}^{-1}$. Mel-Zn_{CV} was collected after 5~cycles of CV and stopped after the oxidation cycle (Figure 1c). The sample was dried at 100°C for 1 h in a vacuum oven and stored in ambient conditions. In the second method, Zn²⁺ loading was performed by immersing melanin (50 mg) into 10 ml solutions of 0.1 and 0.05 M Zn(NO₃)₂ at room temperature for 3 h. After washing twice with dd-H₂O, Zn²⁺ loaded melanin samples (Mel-Zn_{0.1} and Mel-Zn_{0.05}) were dried at 100°C for 1 h in a vacuum oven and stored in ambient conditions.

Materials Characterization: X-ray photoelectron spectroscopy was performed using the Kratos Axis Supra XPS (Axis Supra XPS, Manchester, U.K.). Survey and high-resolution spectra of zinc (Zn) were obtained using an aluminum (Al) source and were further analyzed by CasaXPS software. Elemental analysis was done by determining the peak areas and taking into account the relative sensitivity factors of the instrumentation to individual atomic species.

Raman spectra of Mel and Mel-Zn were collected using an AFM-Raman microscope (NTEGRA Spectra, NT-MDT Spectrum Instruments, Moscow, Russia) with a 10X objective and 500 nm wavelength laser over a Raman shift range of 800 to 2500 cm $^{-1}$. To minimize sample degradation and maximize the signal-to-noise ratio, data from five separate scans using 1 mW of laser power and 10 s exposure time were averaged. Raman peaks were deconvolved using automatic multiple peak fit methods and the Voigt function (Originlab, Northampton, MA USA).

Transmission electron microscopy was performed to analyze the shape and structure of melanin using JEOL JEM 2100 LaB6 (JEM 2100 LaB6, Peabody, MA USA). The particle solution was deposited on a carbon-coated TEM grid (Structure Probe, Inc., West Chester, PA). Once the surface of the grid dried, it was transferred to the TEM grid holder and examined without staining. The acceleration voltage was set to 200 kV. All images were collected via the CCD camera attached to the TEM.

Bacteria Binding Efficiency: The binding of Mel-Zn to bacteria was evaluated using a gram-negative *E. coli* strain (ATCC15 597). Prior to each binding test, *E. coli* was streaked from a frozen glycerol stock onto lysogeny broth (LB) agar. A single colony of *E. coli* was collected from the LB plate and inoculated in 5 mL of LB liquid medium at 37°C in shaking condition. After 15–16 h, bacterial density was determined by the means of optical density (OD) at 600 nm and adjusted to 5×10^5 CFU ml $^{-1}$ (CFU = Colony forming unit). [18] 5 mg of Mel-Zn complexes were inoculated with bacteria suspension in PBS and animal whole blood at 37°C for 1 h in shaking condition. Aliquots of the samples were serially diluted and plated on LB agar for overnight incubation at 37°C. Visible colonies were counted and

www.advancedsciencenews.com



www.advmatinterfaces.de

compared with the negative control which was grown without Mel-Zn to evaluate the bacteria binding efficiencies.

LPS Binding Assay: The Endotoxin binding capacity of Mel-Zn was measured by chromogenic Limulus amoebocyte lysate (LAL) assay (ThermoFisher Scientific, Waltman, MA USA). Briefly, 2, and 10 mg ml $^{-1}$ of Mel-Zn samples were incubated with 1 EU ml $^{-1}$ (EU = endotoxin unit) Escherichia coli LPS endotoxin standard (011: B4) at 37 °C. After 1 h, the remaining endotoxin in the solution was measured by the addition of 50 μ l LAL reagent and 100 μ l chromogenic substrate solution and incubation for 10 and 6 min at 37 °C, respectively. After incubation, 100 ml of the stop reagent (acetic acid, 25% v/v in water) was added, and absorbance was measured at 405 nm on a microplate reader. LPS concentration in the sample solutions was determined using a known standard calibration curve. $^{[53]}$

Protein Recovery: Bovine serum albumin (BSA) was used as a model protein to evaluate protein adsorption by Mel-Zn complexes. Mel and Mel-Zn (5 mg ml $^{-1}$) were incubated with 1000, and 500 BSA at 37 $^{\circ}\text{C}$. After 1 h, BSA concentrations in the solutions were determined using a Pierce BCA protein assay kit (ThermoFisher Scientific, Waltman, MA US). BSA recovery was calculated based on comparing BSA concentration in solution before and after being incubated with Mel or Mel-Zn.

Coagulation Activation: Human Thrombin-Antithrombin Complex (TAT) in vitro enzyme-linked immunosorbent assay (ELISA) (Abcam INC, Waltham, MA USA) was used for quantitative measurement of TAT complex concentrations in plasma. Blood coagulation was characterized by incubating 5 mg Mel and Mel-Zn in 300 µl human whole blood containing heparin as an anticoagulant. After 30 min incubation at 37 °C blood was centrifuged at 3000 g for 10 min and supernatant containing plasma was collected. Standards and plasma samples were added to the wells of a precoated 96-well plate with TAT-specific antibodies and washed with wash buffer after 2 h incubation. Afterward, a TAT-specific biotinylated detection antibody is added and then followed by washing with wash buffer. Next streptavidin-peroxidase conjugate was added, and unbound conjugates were washed away with wash buffer. Chromogen substrate was then used to visualize Streptavidin-Peroxidase enzymatic reaction. Chromogen substrate is catalyzed by Streptavidin-Peroxidase to generate a blue color which changes into yellow after adding an acidic stop solution. The absorbance was measured at a wavelength of 540 nm. TAT concentration in the sample solutions was determined using a known standard calibration

Hemolysis Ratio: To evaluate hemolytic potential, 5 mg of Mel and Mel-Zn were incubated with 1 ml animal red blood cells (2×10^8 cell ml $^{-1}$) for 30 min and then centrifuged at 900 rcf for 5 min to separate the supernatant. The absorbance of the supernatant was measured at a wavelength of 540 nm. PBS solution and distilled water were used as negative (0% lysis) and positive controls (100% lysis), respectively. The hemolysis ratio will be calculated using the following equation (1):

Hemolysis ratio % =
$$\frac{A_s - A_{nc}}{A_{pc} - A_{nc}} \times 100$$
 (1)

where A_s , A_{nc} , and A_{pc} represent absorbance of the samples, negative control, and positive control, respectively.

Statistical Analysis: All data were presented as mean \pm standard deviation (SD). Each result is an average of three parallel experiments. The statistical significance was analyzed using one-way ANOVA. (*p < 0.05, *p < 0.01).

Supporting Information

Supporting Information is available from the Wiley Online Library or from the author.

Acknowledgements

The authors acknowledge the financial support provided by the National Institute of Health (5R21 EB032134-02), National Science Foundation

(NSF) EPSCoR #1757371, and the College of Engineering and Physical Sciences CEPS at the University of New Hampshire. The authors also like to thank the University Instrument Center at UNH.

Conflict of Interest

The authors declare no conflict of interest.

Data Availability Statement

The data that support the findings of this study are available from the corresponding author upon reasonable request.

Keywords

endotoxin, eumelanin, sepsis

Received: May 5, 2023 Revised: November 4, 2023 Published online:

- [1] W. H. Organisation, Global Report on the Epidemiology and Burden of Sepsis: Current Evidence, Identifying Gaps and Future Directions, 2020
- [2] S. A. Asner, F. Desgranges, I. T. Schrijver, T. Calandra, J. Infect. 2021, 82, 125.
- [3] J.-J. Lee, K. J. Jeong, M. Hashimoto, A. H. Kwon, A. Rwei, S. A. Shankarappa, J. H. Tsui, D. S. Kohane, Nano Lett. 2014, 14, 1.
- [4] V. D'onofrio, A. Meersman, K. Magerman, L. Waumans, K. Van Halem, J. A. Cox, J. C. Van Der Hilst, R. Cartuyvels, P. Messiaen, I. C. Gyssens, Int. J. Antimicrob. Agents 2021, 58, 106379.
- [5] M. L. Donnell, A. J. Lyon, M. R. Mormile, S. Barua, Nanotechnology 2016, 27, 285601.
- [6] T. F. Didar, M. J. Cartwright, M. Rottman, A. R. Graveline, N. Gamini, A. L. Watters, D. C. Leslie, T. Mammoto, M. J. Rodas, J. H. Kang, A. Waterhouse, B. T. Seiler, P. Lombardo, E. I. Qendro, M. Super, D. E. Ingber, *Biomaterials* 2015, 67, 382.
- [7] J. H. Kang, M. Super, C. W. Yung, R. M. Cooper, K. Domansky, A. R. Graveline, T. Mammoto, J. B. Berthet, H. Tobin, M. J. Cartwright, A. L. Watters, M. Rottman, A. Waterhouse, A. Mammoto, N. Gamini, M. J. Rodas, A. Kole, A. Jiang, T. M. Valentin, A. Diaz, K. Takahashi, D. E. Ingber, *Nat. Med.* 2014, 20, 1211.
- [8] L. Papafilippou, A. Claxton, P. Dark, K. Kostarelos, M. Hadjidemetriou, Adv. Healthcare Mater. 2021, 10, 2001378.
- [9] I. K. Herrmann, M. Urner, S. Graf, C. M. Schumacher, B. Roth-Z'graggen, M. Hasler, W. J. Stark, B. Beck-Schimmer, Adv. Healthcare Mater. 2013, 2, 829.
- [10] Z. Shi, L. Jin, C. He, Y. Li, C. Jiang, H. Wang, J. Zhang, J. Wang, W. Zhao, C. Zhao, J. Colloid Interface Sci. 2020, 576, 1.
- [11] J. H. Kang, M. Super, C. W. Yung, R. M. Cooper, K. Domansky, A. R. Graveline, T. Mammoto, J. B. Berthet, H. Tobin, M. J. Cartwright, A. L. Watters, M. Rottman, A. Waterhouse, A. Mammoto, N. Gamini, M. J. Rodas, A. Kole, A. Jiang, T. M. Valentin, A. Diaz, K. Takahashi, D. E. Ingber, Nat. Med. 2014, 20, 1211.
- [12] A. Bicart-See, M. Rottman, M. Cartwright, B. Seiler, N. Gamini, M. Rodas, M. Penary, G. Giordano, E. Oswald, M. Super, D. E. Ingber, PLoS One 2016, 11, e0156287.
- [13] L. Panzella, G. Gentile, G. D'errico, N. F. Della Vecchia, M. E. Errico, A. Napolitano, C. Carfagna, M. D'ischia, Angew. Chem. Int. Ed. 2013, 52, 12684.

ADVANCED SCIENCE NEWS

www.advancedsciencenews.com



www.advmatinterfaces.de

- [14] A. A. R. Watt, J. P. Bothma, P. Meredith, Soft Matter 2009, 5, 3754.
- [15] W. Xie, E. Pakdel, Y. Liang, Y. J. Kim, D. Liu, L. Sun, X. Wang, Biomacromolecules 2019, 20, 4312.
- [16] P. Meredith, T. Sarna, Pigment Cell Res. 2006, 19, 572.
- [17] Z. Tian, W. Hwang, Y. J. Kim, J. Mater. Chem. B 2019, 7, 6355.
- [18] T. Rahmani Eliato, J. T. Smith, Z. Tian, E.-S. Kim, W. Hwang, C. P. Andam, Y. J. Kim, J. Mater. Chem. B 2021, 9, 1536.
- [19] Y. J. Kim, W. Wu, S.-E. Chun, J. F. Whitacre, C. J. Bettinger, Proc. Natl. Acad. Sci. USA 2013, 110, 20912.
- [20] Y. J. Kim, W. Wu, S.-E. Chun, J. F. Whitacre, C. J. Bettinger, Adv. Mater. 2014, 26, 6572.
- [21] C. Pitchumani Violet Mary, R. Shankar, S. Vijayakumar, Mol. Simul. 2019, 45, 636.
- [22] V. Ganesh, K. Bodewits, S. J. Bartholdson, D. Natale, D. J. Campopiano, J. C. Mareque-Rivas, Angew. Chem. Int. Ed. 2009, 48, 356.
- [23] H. T. Ngo, X. Liu, K. A. Jolliffe, Chem. Soc. Rev. 2012, 41, 4928.
- [24] R. G. Hanshaw, C. Lakshmi, T. N. Lambert, J. R. Johnson, B. D. Smith, ChemBioChem 2005, 6, 2214.
- [25] A. D. Cabral, N. Rafiei, E. D. De Araujo, T. B. Radu, K. Toutah, D. Nino, B. I. Murcar-Evans, J. N. Milstein, D. Kraskouskaya, P. T. Gunning, ACS Sens. 2020, 5, 2753.
- [26] E. J. O'neil, B. D. Smith, Coord. Chem. Rev. 2006, 250, 3068.
- [27] L. Mazgaeen, P. Gurung, Int. J. Mol. Sci. 2020, 21, 379.
- [28] P. de Oliveira Magalhães, A. M. Lopes, P. G. Mazzola, C. Rangel-Yagui, T. C. V. Penna, A. Pessoa, J. Pharm. Pharm. Sci. 2007, 10, 388.
- [29] C. Wang, J. Bendle, Y. Yang, H. Yang, H. Sun, J. Huang, S. Xie, Org. Geochem. 2016, 94, 21.
- [30] E. T. Rietschel, T. Kirikae, F. U. Schade, U. Mamat, G. Schmidt, H. Loppnow, A. J. Ulmer, U. Zähringer, U. Seydel, F. Di Padova, M. Schreier, H. Brade, FASEB J. 1994, 8, 217.
- [31] S. Supakar, A. Banerjee, T. Jha, Comput. Theor. Chem. 2019, 1151, 43.
- [32] E. Kaxiras, A. Tsolakidis, G. Zonios, S. Meng, Phys. Rev. Lett. 2006, 97, 218102
- [33] C.-T. Chen, C. Chuang, J. Cao, V. Ball, D. Ruch, M. J. Buehler, Nat. Commun. 2014, 5, 3859.

- [34] C.-T. Chen, V. Ball, J. J. De Almeida Gracio, M. K. Singh, V. Toniazzo, D. Ruch, M. J. Buehler, ACS Nano 2013, 7, 1524.
- [35] H. Lee, N. F. Scherer, P. B. Messersmith, Proc. Nat. Acad. Sci. 2006, 103, 12999.
- [36] A. H. Mishra, D. Mishra, Biomacromolecules 2020, 21, 688.
- [37] A. I. A. Soliman, A. M. A. Abdel-Wahab, H. N. Abdelhamid, RSC Adv. 2022, 12, 7075.
- [38] H.-A. Park, Y. J. Kim, I. S. Kwon, L. Klosterman, C. J. Bettinger, *Polym. Int.* 2016, 65, 1331.
- [39] A. C. Ferrari, Solid State Commun. 2007, 143, 47.
- [40] M. Yoshikawa, N. Nagai, M. Matsuki, H. Fukuda, G. Katagiri, H. Ishida, A. Ishitani, I. Nagai, Phys. Rev. B 1992, 46, 7169.
- [41] H. H. Dolin, T. J. Papadimos, X. Chen, Z. K. Pan, Microbiol. Insights 2019, 12, 1178636118825081.
- [42] J. Dien Bard, E. Mcelvania Tekippe, J. Clin. Microbiol. 2016, 54, 1418.
- [43] T. Reier-Nilsen, T. Farstad, B. Nakstad, V. Lauvrak, M. Steinbakk, BMC Pediatr. 2009, 9, 5.
- [44] P. Yagupsky, F. S. Nolte, Clin. Microbiol. Rev. 1990, 3, 269.
- [45] N. Jacob Kaleekkal, J. Memb. Sci. 2021, 623, 119068.
- [46] K. Zhao, R. Lin, W. Chen, Z. Li, K. Wu, B. Guan, Y. Jiao, C. Zhou, Composites Communications 2020, 20, 100365.
- [47] G. Tatra, A. Reinthaller, Klin. Wochenschr. 1991, 69, 124.
- [48] X.-C. Peng, W.-D. Yang, J.-S. Liu, Z.-Y. Peng, S.-H. Lu, W.-Z. Ding, J. Integr. Plant Biol. 2005, 47, 165.
- [49] A. Banerjee, A. Kunwar, B. Mishra, K. I. Priyadarsini, Chem. Biol. Interact 2008, 174, 134
- [50] C. Wang, X. Qin, B. Huang, F. He, C. Zeng, Biochem. Biophys. Res. Commun. 2010, 402, 773.
- [51] C. Amri, M. Mudasir, D. Siswanta, R. Roto, Int. J. Biol. Macromol. 2016. 82, 48.
- [52] L. P. Amarnath, A. Srinivas, A. Ramamurthi, Biomaterials 2006, 27, 1416.
- [53] Y. Li, Z. Shi, I. Radauer-Preiml, A. Andosch, E. Casals, U. Luetz-Meindl, M. Cobaleda, Z. Lin, M. Jaberi-Douraki, P. Italiani, J. Horejs-Hoeck, M. Himly, N. A. Monteiro-Riviere, A. Duschl, V. F. Puntes, D. Boraschi, *Nanotoxicology* 2017, 11, 1157.